AN ABSTRACT OF THE THESIS OF

MICHAEL ARTHUR LIPPARELLI for the Ph. D.
(Name) (Degree)

in General Science (Physical Science) presented on June 22, 1970
(Major) (Date)

Title: The GEK Signatures of Lowest Mode Internal Waves

Abstract approved: Redacted for Privacy
George F. Beardsley, Jr.

Present GEK (Geomagnetic Electrokinetograph) theory is extended to include internal waves of the lowest mode. The predicted towed electrode GEK signal is determined to second-order for long-crested internal waves in a finite but deep ocean. The analysis includes the determination of GEK signatures for small amplitude and finite amplitude interfacial waves along shallow thermoclines. In addition, the GEK response to internal waves existent in a continuously stratified fluid is discussed along with a particular application of the GEK theory to internal waves in a sea possessing a density profile of the form $\rho_0 = \rho_0(0)(1-\mu z)$. The validity of the theory is restricted to waves within the wave number range $k = 10^{-4}$ m^{-1} to $k = 10$ m^{-1} due to the assumption that the electric currents associated with time variations in the induced magnetic field be negligible.

The results indicate that internal waves of reasonable amplitude would produce a detectable signal at mid and high

latitudes, but would be undetectable at low latitudes. The vertical component of the Earth's magnetic field, H_z, and the wave amplitude are shown to have the dominant effect in determining the magnitude of the GEK signal. For fixed latitude and wave number, the interfacial wave GEK signal increases as the depth of the thermocline decreases. Similarly for fixed latitude and thermocline depth, the signal increases as the wave number k decreases. As the density difference across the thermocline increases, the GEK response will increase. Corresponding relationships exist for continuous density internal wave GEK values but are found to be less influential.

Finally, internal standing waves are shown to produce no detectable signal voltages. A discussion of experimental precautions necessary in the GEK monitoring of internal waves is also included.

The GEK Signatures of Lowest Mode Internal Waves

by

Michael Arthur Lipparelli

A THESIS

submitted to

Oregon State University

in partial fulfillment of
the requirements for the
degree of

Doctor of Philosophy

June 1971

APPROVED:

Redacted for Privacy

Associate Professor of Oceanography
in charge of major

Redacted for Privacy

Chairman of the Department of General Science

Redacted for Privacy

Dean of Graduate School

Date thesis is presented June 22, 1970

Typed by Muriel Davis for Michael Arthur Lipparelli

TABLE OF CONTENTS

TABLE OF CONTENTS (continued)

LIST OF FIGURES

LIST OF TABLES

THE GEK SIGNATURES OF LOWEST MODE INTERNAL WAVES

CHAPTER I

INTRODUCTION

During the January, February, 1969 YALOC cruise to the Panama Basin large sinusoidal fluctuations were observed in the towed electrode GEK (Geomagnetic Electrokinetograph) signals. These reoccurring variations typically exhibited a periodicity of order two minutes with an amplitude of two millivolts, which is a large fluctuation when compared to a normal signal which contains periods of a few seconds. The sinusoidal periodicity of these signals coupled with the absence of significant surface waves at the time of their recording led to the consideration of internal waves as a possible cause. The use of GEK apparatus for the measuring of velocity fields in the ocean, particularly for ocean currents and surface waves, is well established. Therefore, it is the purpose of this thesis to extend these techniques to include internal waves and to provide the theoretical development necessary to interpret internal wave GEK data.

In Chapter II the GEK response to two-dimensional, long-crested interfacial waves of the lowest mode along a shallow thermocline is discussed for small amplitude and finite amplitude wave cases. Numerical examples are provided for small amplitude waves at

various thermocline depths. The general characteristics of the internal wave GEK signatures are then deduced through an examination of the tabulated results. The GEK theory and corresponding signatures of finite amplitude waves are developed in a similar manner. Chapter III presents the theoretical derivation of the GEK response to two-dimensional, long-crested internal waves in continuously stratified media. A specific application is given for internal waves existent in a density profile of the form $\rho_0 = \rho_0(0)(1-\mu z)$. Continuous density standing internal waves are considered in Chapter IV and are shown to produce no detectable signal voltages.

Previous Investigations

Michael Faraday (1832) was the first to consider induced fields in the ocean. His theoretical prediction of their existence was confirmed when tidally induced potentials were observed in broken submarine cables along the English Channel. Experimental cable measurements around the British Isles continued for many years. The history of these investigations is well summarized in Longuet-Higgins (1949). The more recent of this type of cable work are Longuet-Higgins (1947), Barber (1948), Barber and Longuet-Higgins (1948) Bowden (1956), and Bowden and Hughes (1961).

While submarine cable voltages were being monitored and interpreted, techniques were developed to serve areas where no cables

were available. Young, Gerard, and Jevons (1920) proposed the use of towed and moored electrode pairs. Shortly thereafter, Williams (1930) and Kolin (1944) began their attempts to develop functional flow meters for application to blood flow velometry. It was not until Longuet-Higgins (1949) and Stommel (1948), however, that the relevant theory was supplied for the oceanographic application of these devices. Combining the results of these theoretical studies and operational techniques, von Arx (1950) established the method of towed electrodes more commonly known as GEK. Experimental GEK treatments rapidly followed. Comparisons between GEK measurements and the Loran dead-reckoning method were made for velocity fields in the Gulf Stream (von Arx, 1952). Wind drift currents were measured by Bowden (1953) in the North Channel. Vaux (1955) applied towed electrode techniques to tidal streams in shallow water and compared the findings with existing tidal stream data.

The first major refinement of von Arx's work of 1950 was provided by Longuet-Higgins, Stern, and Stommel (1954). They extended the theory to include surface waves and calculated the GEK response to several specific velocity profiles. Malkus and Stern (1952) proved two integral theorems linking GEK measurements to the total transport of ocean currents. This allowed Wertheim (1954) and Richardson and Schmitz (1965) to estimate the transport of the Florida Current. Simultaneously, towed electrode experimentation was continued by

Chew (1958) and Morse et al. (1958).

The comparison of drogue measurements and GEK measurements by Reid (1958) and a paper on the effects of cable design by Knauss and Reid (1957) set the standard for the correct experimental interpretation of GEK data. Mangelsdorf (1962) and Konaga (1964) were likewise concerned with accounting for and minimizing external influences that could affect GEK readings. The effects of telluric currents and geomagnetic variations on GEK signals have received extensive treatment as they are a major source of potential interference (Fonarev, 1961a, 1961b, 1961c; Novysh and Fonarev, 1963; Ivanov and Kostomarov, 1963; Runcorn, 1964; Fonarev, 1964; Fonarev and Novysh, 1965; Novysh, 1965; Novysh and Fonarev, 1966; and Fonarev, 1968). Similarly, Hughes (1962) has reviewed the GEK effect of sea bed conductivity in shallow water while Chew (1967) has examined the cross-stream variation of the k-factor used in converting GEK observations to current speeds. The overall objective of these works is to provide greater accuracy in GEK methods.

The most recent GEK investigations have been concerned with two- and three-dimensional flows. Tikhonov and Sveshnikov (1959) and Glasko and Sveshnikov (1961) examine the electric fields induced by two-dimensional steady flows whereas Fonarev (1963) looks at the vertical electric currents in a two-dimensional sea. Larsen (1966) in a thesis and later in Larsen and Cox (1966) shows that the magnetic

effects of tidally induced electric currents can be significant in the open ocean. Extension of GEK theory to three-dimensional quasi-steady flows is presented in Sanford (1967) along with his experimental vertical GEK measurements of the Gulf Stream.

Finally, it should be mentioned that the Soviet Union has maintained a parallel program of analysis of geomagnetically induced marine electric currents. The towed electrode counterpart of the GEK is known as EMIT. Its experimental operation along with pertinent data analysis techniques can be found in Sysoev and Volkov (1957), Moroshkin (1957), Bogdanov and Ivanov (1960), Solov'yev (1961), and Gorodnicheva (1966).

General Principles of Towed Electrode GEK

The method of towed electrodes is based on the following electromagnetic theory. Faraday's Law of Induction states that if a simple closed circuit C moves through a magnetic field $\underline{B}$ an electromotive force, E, will be induced in C according to the equation:

$$E = -\frac{d\Phi}{dt} \tag{1.1}$$

where Φ = magnetic flux through C. This change in flux may be due to either a time rate of change in the magnetic field or a movement of the circuit or both. Let us assume that $\underline{B}$ is constant. Then, the rate of change of flux through C due to circuit motion is equal to

the rate at which the circuit cuts lines of flux. If we consider an element $d\underline{\ell}$ of the circuit C moving with velocity $\underline{v}$ (see Figure 1), it sweeps out in time dt an area whose projection in the direction of $\underline{B}$ is $(\underline{v}\, dt \times d\underline{\ell}) \cdot \underline{B}$. According to Figure 1, this equals $-\underline{v} \times \underline{B} \cdot d\underline{\ell}\, dt$. Summing up all elements $d\underline{\ell}$ in C, the rate of cutting lines of magnetic flux per unit time dt is:

$$\frac{d\Phi}{dt} = \oint_C - \underline{v} \times \underline{B} \cdot d\underline{\ell} \ . \tag{1.2}$$

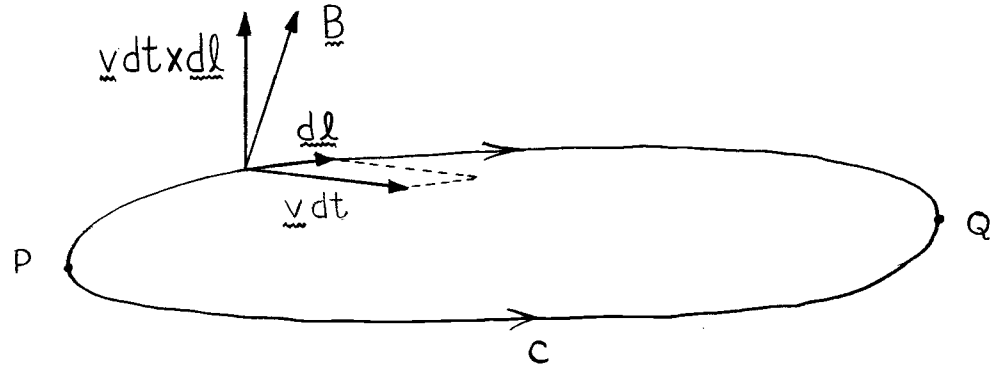

Figure 1. Towed electrode schematic diagram.

Therefore, equation (1.1) becomes

$$E = \oint_C \underline{v} \times \underline{B} \cdot d\underline{\ell} \ . \tag{1.3}$$

In a continuous conducting media, an induced e.m.f. would cause a current density $\underline{i}$ to flow along an arbitrary path C

according to Ohm's Law:

$$\underset{\sim}{E} = \rho \underset{\sim}{i} \tag{1.4}$$

where ρ is the resistivity of the media. If this e.m.f. is due solely to $\underset{\sim}{v} \times \underset{\sim}{B}$, we have:

$$\oint_C (\underset{\sim}{v} \times \underset{\sim}{B} - \rho \underset{\sim}{i}) \cdot \underset{\sim}{d\ell} = 0. \tag{1.5}$$

We can now define an electrostatic scalar potential ϕ, at each point P in space (see Figure 1):

$$\phi(P) = \int_Q^P (\underset{\sim}{v} \times \underset{\sim}{B} - \rho \underset{\sim}{i}) \cdot \underset{\sim}{d\ell} \ . \tag{1.6}$$

The path of integration is arbitrary provided the integral around a closed circuit is zero. From equation (1.6), this may be written as:

$$\underset{\sim}{\nabla \phi} = \underset{\sim}{v} \times \underset{\sim}{B} - \rho \underset{\sim}{i}. \tag{1.7}$$

The potential ϕ is the same as would be measured by a stationary potentiometer connected between Q and P.

Suppose the potentiometer consists of a wire circuit C (see Figure 1) which contains a voltage cell with voltage E_c. Further assume that the voltage cell is located in the area denoted by the letter C and is so adjusted as to reduce the current in the segment PCQ to zero. Then the total e.m.f. for any circuit C is:

$$E_c = \int_{PQ} (\underset{\sim}{v} \times \underset{\sim}{B} - \rho \underset{\sim}{i}) \cdot \underset{\sim}{d\ell} \qquad (1.8)$$

where PQ is the upper segment of the circuit C. From equation (1.6), this is written as:

$$E_c = \phi(P). \qquad (1.9)$$

If the potentiometer is also in motion with velocity $\underset{\sim}{v}$, then the PCQ contribution is finite and equation (1.9) becomes:

$$E = \phi(P) - \int_{PCQ} (\underset{\sim}{v} \times \underset{\sim}{B}) \cdot \underset{\sim}{d\ell}\,. \qquad (1.10)$$

By taking P sufficiently close to Q, we might obtain the potential gradient at Q. For stationary electrodes we would have:

$$E = \phi(P) - \phi(Q) = \nabla\phi \cdot \underset{\sim}{PQ}, \qquad (1.11)$$

and for moving electrodes:

$$E = (\nabla\phi - \underset{\sim}{v} \times \underset{\sim}{B}) \cdot \underset{\sim}{PQ}. \qquad (1.12)$$

Thus E would be the apparent gradient measured by a recording system attached at Q and P.

The Method of Towed Electrodes

Suppose the two electrodes are towed in a line behind a ship. Assuming the velocity of the water to be $\underset{\sim}{v}$ for both the ship and the

electrodes, we will denote the velocity of the ship relative to the water to be $\underset{\sim}{v}_l$, which is written as:

$$\underset{\sim}{v}_l = \underset{\sim}{v}_p + \underset{\sim}{v}_w \tag{1.13}$$

where $\underset{\sim}{v}_p$ = velocity due to the ship's propellors and $\underset{\sim}{v}_w$ is the additional velocity due to the wind. The absolute velocity of the ship in a steady state is then:

$$\underset{\sim}{v} + \underset{\sim}{v}_l . \tag{1.14}$$

Since the electrodes are in motion with velocity $\underset{\sim}{v}+\underset{\sim}{v}_l$, the voltage that they will record will be by equation (1.12):

$$(\nabla\underset{\sim}{\phi} - (\underset{\sim}{v} + \underset{\sim}{v}_l) \times \underset{\sim}{B}) \cdot \underset{\sim}{PQ} . \tag{1.15}$$

Since the vector $\underset{\sim}{PQ}$ is parallel to $\underset{\sim}{v}_l$, we have

$$\underset{\sim}{v}_l \times \underset{\sim}{B} \cdot \underset{\sim}{PQ} = 0 , \tag{1.16}$$

which says that the electrode line itself is not cutting any lines of magnetic flux as it is towed. Thus, equation (1.15) becomes:

$$(\nabla\underset{\sim}{\phi} - \underset{\sim}{v} \times \underset{\sim}{B}) \cdot \underset{\sim}{PQ} . \tag{1.17}$$

However, $$\nabla\underset{\sim}{\phi} = \underset{\sim}{v} \times \underset{\sim}{B} - \rho\underset{\sim}{i} . \tag{1.18}$$

Therefore, equation (1.17) reduces to:

$$-\rho\underset{\sim}{i} \cdot \underset{\sim}{PQ} . \tag{1.19}$$

The electrodes thus measure the component of the electrical current density $-\rho \underset{\sim}{i}$ in the direction of the electrode line PQ.

In certain special cases, the potential gradient may be shorted out by the presence of a conducting boundary such as the sea bed or nearby motionless water layers. Then we have:

$$\nabla \underset{\sim}{\phi} = 0, \tag{1.20}$$

whereby

$$\rho \underset{\sim}{i} = \underset{\sim}{v} \times \underset{\sim}{B}. \tag{1.21}$$

Hence the recorded voltage will be:

$$- \underset{\sim}{v} \times \underset{\sim}{B} \cdot \underset{\sim}{PQ}, \tag{1.22}$$

which represents a direct measure of the component velocity at right angles to the electrode line.

Equations (1.13) through (1.22) constitute the theory known as the method of towed electrodes or the Geomagnetic Electrokinetograph (GEK). It was originally derived by Longuet-Higgins, Stern and Stommel (1954).

CHAPTER II

GEK RESPONSE TO TWO-DIMENSIONAL INTERFACIAL INTERNAL WAVES

Introduction

In this chapter the theory of the towed electrode GEK is extended to include two-dimensional interfacial internal waves. The predicted GEK response to such waves in the deep ocean is then determined for two specific cases. The first concerns the GEK signature of small amplitude internal waves of the lowest mode along a shallow thermocline. The second case examines the GEK signatures of finite amplitude interfacial waves of the lowest mode along a deep ocean density discontinuity. In both examples, the GEK signals are reviewed in terms of the effects of varying parameters such as thermocline depth, density difference, and wave number. Numerical calculations are provided for the small amplitude wave situation.

GEK Theory for Two-dimensional Interfacial Waves

As indicated in Chapter I, the towed electrode GEK signal is determined by solving the electromagnetic field equations and boundary conditions related to the particular wave system under investigation. For the two-dimensional interfacial internal waves to be considered later, the wave system will be assumed to exist in the

following theoretical model from which the field equations are derived.

Consider a laterally unbounded ocean of finite yet great depth. The water in this sea will consist of two layers of sea water of different density. To distinguish the two layers of fluid, we will use primed symbols for the upper layer and double primed symbols for the lower layer. The density and resistivity of each layer will be assumed to be constant. The ocean is bounded at depth $z = -h''$ by the sea floor and has a free surface at $z = h'$. The sea bed will be taken to possess such low conductivity as to be considered an insulator. The origin of the axes lies on the undisturbed fluid interface which corresponds to the natural phenomenon of a sharp thermocline. The internal waves will be assumed to be infinitely long-crested in the y-direction and travelling in the positive x-direction. The motion in the system will be restricted solely to that due to internal waves of the lowest mode along the fluid interface as shown in Figure 2. The velocity of motion will be small compared to the speed of light allowing us to neglect free charges and displacement currents. The external magnetic field is to be steady and uniform.

Faraday's Law of Induction and Ohm's Law require of such a system moving in a uniform magnetic field that:

$$\nabla\phi = \underset{\sim}{v} \times \underset{\sim}{B} - \rho \underset{\sim}{i} - \frac{\partial \underset{\sim}{A}}{\partial t}, \qquad (2.1)$$

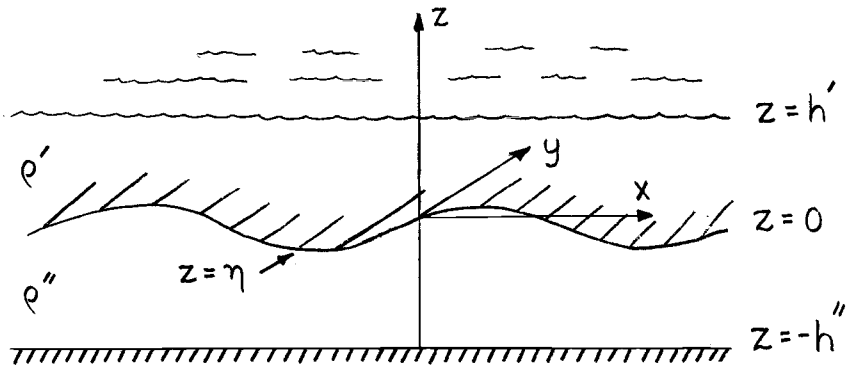

Figure 2. Interfacial wave geometry.

where ϕ = electric scalar potential, $\underset{\sim}{v}$ = velocity of the fluid, $\underset{\sim}{B}$ = magnetic field, ρ = electrical resistivity of sea water, $\underset{\sim}{i}$ = electric current density, and $\underset{\sim}{A}$ = magnetic vector potential.

The time-dependent component of the flow will be assumed to be small compared to the electromagnetic skin depth in the ocean (see Appendix I). This restriction, although it limits the wave number range for which the theory is valid, allows us to neglect $\partial \underset{\sim}{A}/\partial t$ as compared to $\nabla \phi$. Equation (2.1) thereby reduces to

$$\nabla \phi = \underset{\sim}{v} \times \underset{\sim}{B} - \rho \underset{\sim}{i}. \tag{2.2}$$

Conservation of electric charge is to be maintained and is given as

$$\nabla \cdot \underset{\sim}{i} = 0. \tag{2.3}$$

For the two-layered ocean, the related boundary conditions to be imposed are:

(a) in the absence of magnetic material

$$\nabla \cdot \underset{\sim}{B} = 0, \tag{2.4}$$

(b) we will assume the sea to possess uniform electrical conductivity in each layer, then

$$\nabla \rho = 0, \tag{2.5}$$

(c) at a physical boundary or a surface of discontinuity (excepting the fluid interface), the normal component of the electric current density must vanish

$$[\underset{\sim}{i} \cdot \underset{\sim}{n}]_1^2 = 0 \tag{2.6}$$

where $\underset{\sim}{n}$ is the unit vector normal to the surface and the suffixes 1 and 2 denote the two sides of the surface.

Taking the divergence of both sides of equation (2.2) and imposing equations (2.3) through (2.6) we get:

$$\nabla^2 \phi = \underset{\sim}{B} \cdot \nabla \times \underset{\sim}{v}, \tag{2.7}$$

which is the governing equation for induced fields in the sea. It should be noted that in a region where the velocity distribution is zero, such as above the sea surface or below the ocean bottom, equation (2.7) reduces to Laplace's equation:

$$\nabla^2 \phi = 0. \tag{2.8}$$

It is now necessary to solve these electromagnetic field equations for two-dimensional internal wave motion. Divide the magnetic field into two parts, one parallel and one perpendicular to the y-axis.

$$\underset{\sim}{B} = \underset{\sim}{B}_1 + \underset{\sim}{B}_2 \tag{2.9}$$

where

$$\underset{\sim}{B}_1 = (0, H_y, 0) \quad \text{and} \quad \underset{\sim}{B}_2 = (H_x, 0, H_z). \tag{2.10}$$

The solutions ϕ and $\underset{\sim}{i}$ corresponding to $\underset{\sim}{B}_1$ and $\underset{\sim}{B}_2$ will be denoted by suffixes 1 and 2. The internal wave is long-crested allowing us to set the y-component of velocity equal to zero. Thus:

$$\underset{\sim}{v} = (u, 0, w) = \left(-\frac{\partial \psi}{\partial z}, 0, \frac{\partial \psi}{\partial x}\right) \tag{2.11}$$

where use has been made of the general relationship between the velocity components u and w, stream functions ψ, and velocity-potential functions Φ:

$$\frac{\partial \Phi}{\partial x} = \frac{\partial \psi}{\partial z} = -u, \qquad \frac{\partial \Phi}{\partial z} = -\frac{\partial \psi}{\partial x} = -w. \tag{2.12}$$

Considering the field due to $\underset{\sim}{B}_1$, we have from equation (2.2) that:

$$\rho \underset{\sim}{i}_1 = \underset{\sim}{v} \times \underset{\sim}{B}_1 - \nabla \underset{\sim}{\phi}_1 = \nabla(-H_y \psi - \phi_1). \tag{2.13}$$

We now enforce the field equation (2.7) and the boundary conditions (2.3) through (2.6) on equation (2.13) insuring in addition that the vertical current density is continuous across the fluid density

interface. For an internal wave, we obtain the solutions:

$$\underset{\sim}{i}_1 = 0 \quad , \qquad \phi_1 = -H_y \psi \tag{2.14}$$

for each region.

Similarly in considering the contribution due to $\underset{\sim}{B}_2$ we have:

$$\underset{\sim}{v} \times \underset{\sim}{B}_2 = \left(0, H_x \frac{\partial \psi}{\partial x} + H_z \frac{\partial \psi}{\partial z}, 0\right) . \tag{2.15}$$

This is a vector independent of y yet parallel to the y-axis which tends to make current flow in that direction. The current flows freely in the absence of boundaries, and the potential gradient reduces to zero. The solution to the field equation and boundary conditions for $\underset{\sim}{B}_2$ is thus:

$$\rho \underset{\sim}{i}_2 = \left(0, H_x \frac{\partial \psi}{\partial x} + H_z \frac{\partial \psi}{\partial z}, 0\right) , \quad \phi_2 = 0 . \tag{2.16}$$

It should be noted that the existence of a path for the free flow of electric current to infinity in the y-direction as permitted by infinitely long-crested waves is mandatory to produce the derived results. Longuet-Higgins, Stern, and Stommel (1954) point out in their discussion of surface waves that, if this condition is not fulfilled, an additional current density $\underset{\sim}{i}'$ will be superposed on $\underset{\sim}{i}_2$.

Adding equations (2.14) and (2.16), we obtain the current densities and electrical potentials induced in the sea by an interfacial internal wave:

$$\phi' = -H_y \psi' \tag{2.17}$$

$$\phi'' = -H_y \psi'' \tag{2.18}$$

$$\rho \underset{\sim}{i}' = \left(0, H_x \frac{\partial \psi'}{\partial x} + H_z \frac{\partial \psi'}{\partial z}, 0\right), \tag{2.19}$$

$$\rho \underset{\sim}{i}'' = \left(0, H_x \frac{\partial \psi''}{\partial x} + H_z \frac{\partial \psi''}{\partial z}, 0\right). \tag{2.20}$$

Of particular interest is the voltage measured by towed electrodes at the sea surface as the internal wave passes underneath. From Chapter I, we have that the

$$\text{GEK Signal} = \int_P^Q \rho \underset{\sim}{i} \cdot d\underset{\sim}{\ell} = \rho i \, PQ \Big|_{z=h'} \tag{2.21}$$

where the path of integration is along the cable between the tandem electrodes P and Q. Note from equation (2.14) that the component of $\underset{\sim}{i}$ in the plane of motion is zero. Hence, electrodes towed in the direction of propagation of the waves would record zero voltage. Electrodes towed parallel to the crests, however, would record a maximum signal due to the parallel component of $\underset{\sim}{i}$ at the sea surface as given in equation (2.19). Ship headings in different directions in relation to the wave crests will produce reduced signals (see Appendix VI). Specific interfacial internal wave GEK signatures can now be derived by first determining the associated velocity distributions.

Small Amplitude Internal Waves

Literature Summary

The theoretical investigation of progressive small amplitude interfacial waves was begun by Stokes (1847). He was interested in describing the motion induced by gravity waves in a stably stratified, inviscid and incompressible fluid. This work was refined shortly thereafter by Greenhill (1887), Burnside (1889), and Love (1891). Their efforts, however, were focused primarily on evaluating motions in given multi-layered density profiles. It was not until Fjeldstadt (1933) that multi-layered theory was extended to include continuous density profile situations. He demonstrated that for a general density profile the solutions for infinitesimal waves may be expressed in terms of an eigenfunction of a certain Sturm-Liouville equation. Heyna and Groen (1958) expanded on these ideas and proved that the frequency of the infinitesimal waves has an upper bound, known as the Brunt-Vaisala frequency. Yih (1960a) and Yanowitch (1962) went on to examine the properties of the eigenfunctions and related eigenvalues. Meanwhile, exact solutions to continuous density profiles have been explored by Long (1953) and Yih (1960b). Krauss (1964) has compared the exponential density approximation of a continuous density profile to a two-layer approximation of the same system.

The application of many of these theories in the study and interpretation of oceanic phenomena is just beginning. Defant (1950), Haurwitz (1950), and Rattray (1957) have all been concerned with the origin, propagation, and characteristics of long internal tidal waves. In fact, most of the interest is centered on long internal waves since they are so readily detectable. Short internal waves, on the other-hand, have been temporarily neglected due to the complicating effects of turbulence and ocean currents on their theoretical definition and experimental detection. Krauss (1961) and Magaard (1965) have, however, initiated theoretical work on short internal waves. Defant (1961) and La Fond (1962) both present well-rounded expositions on the experimental and theoretical advances in oceanographic studies of internal waves of various types. A general bibliography on internal waves in the sea is to be found in Lee (1965).

Small Amplitude Internal Wave Theory

The equations of motion for infinitesimally small amplitude waves are defined in terms of the theoretical model used. As described previously in this chapter, we will consider interfacial waves in the model as shown in Figure 2. This two-layered ocean will have a free surface. The disturbance along the interface will be assumed to be long-crested, moving in the positive x-direction, and of the form

$$\eta = a \cos(kx - \sigma t) \tag{2.22}$$

where a = amplitude, $k = 2\pi/L$ = wave number, and $\sigma = ck$ = angular frequency. We will insist that the fluid is incompressible

$$\nabla \cdot \underset{\sim}{v} = 0. \tag{2.23}$$

This assumption allows that in two-dimensional motion, we can define a stream function ψ related to the flow as defined in equation (2.12). At this point, we have satisfied the one condition on any internal wave system (that a stream function ψ exists) as set forth by the previously derived interfacial wave GEK theory.

Let us further assume that the motion be irrotational

$$\nabla \times \underset{\sim}{v} = 0. \tag{2.24}$$

This assumption provides for the definition of a velocity-potential function Φ. Under these conditions, the stream function ψ and the velocity-potential function Φ must also satisfy Laplace's equation in both fluid layers as follows:

$$\nabla^2\psi' = \nabla^2\Phi' = 0 \ , \qquad \nabla^2\psi'' = \nabla^2\Phi'' = 0 . \tag{2.25}$$

We now apply the small amplitude approximation (see Phillips, 1966) wherein terms in the Navier-Stokes equations of higher than first-order with respect to wave slope are neglected. Correspondingly, the boundary conditions reduce to first-order (see Appendix II). The kinematic boundary conditions associated with equation (2.25) are to first-order:

$$\frac{\partial \Phi}{\partial \underset{\sim}{n}} = 0 \qquad \text{at a fixed boundary;} \tag{2.26}$$

$$\frac{\partial \eta}{\partial t} = - \left[\frac{\partial \Phi}{\partial z}\right]_{z=0} \qquad \text{at the interface.} \tag{2.27}$$

The dynamic boundary conditions require

$$\rho' \left(\frac{\partial \Phi_1'}{\partial t} - g\eta_1 \right)_{z=0} = \rho'' \left(\frac{\partial \Phi_1''}{\partial t} - g\eta_1 \right)_{z=0} \tag{2.28}$$

at the fluid interface and that at the sea surface

$$\sigma^2 \Phi' = g \frac{\partial \Phi'}{\partial z} \tag{2.29}$$

where g = gravitational acceleration, ρ = density of the fluid in the respective layers, and σ^2 = the square of the angular frequency.

The velocity-potential functions which solve the Laplace's equations (2.25) and the given boundary conditions (2.26) through (2.29) are shown in Lamb (1945, Art. 231) to be:

$$\Phi' = \left\{ \left[- \frac{\rho''}{\rho'} \text{ ca coth } kh'' + \frac{ga}{\sigma} \frac{(\rho''-\rho')}{\rho'} \right] \cosh kz \right.$$

$$\left. - \text{ ca sinh } kz \right\} \sin (kx - \sigma t), \tag{2.30}$$

$$\Phi'' = - \text{ca} \frac{\cosh k(z+h'')}{\sinh kh''} \sin (kx - \sigma t), \tag{2.31}$$

where the square of the angular frequency is:

$$\sigma^2 = \frac{(\rho'' - \rho') gk}{\rho'' \coth kh' + \rho'}, \tag{2.32}$$

and the ocean is deep:

$$\coth kh'' = 1 . \tag{2.33}$$

Knowing equation (2.12), we can readily determine the stream functions ψ and the velocity components u, w for each layer as needed.

GEK Signature

Armed with knowledge of the velocity distribution for an infinitesimal interfacial internal wave, apply equation (2.30) to equations (2.12), (2.19), and (2.21). The resulting GEK signature is:

$$\begin{aligned} GEK = \{ [\frac{k\rho''}{\rho'} ca \coth kh'' - \frac{ga}{c} \frac{(\rho''-\rho')}{\rho'}] \sinh kh' + \\ kac \cosh kh' \} H_x \ell \sin(kx - \sigma t) + \\ \{ [\frac{k\rho''}{\rho'} ca \coth kh'' - \frac{ga}{c} \frac{(\rho''-\rho')}{\rho'}] \cosh kh' + \\ kac \sinh kh' \} H_z \ell \cos(kx - \sigma t) \end{aligned} \tag{2.34}$$

where ℓ = length PQ, ρ = density, k = wave number $= 2\pi/L$, and $c = \sigma/k$.

Table 1 lists the periods and expected values of the H_z GEK component for a one meter amplitude interfacial wave as predicted by equation (2.34). The values are presented for the H_z component according to wave number k, depth of thermocline h', and density difference across the thermocline $\Delta\rho$. Each calculation was made

Table 1. Calculated H_z-Component Periods and Amplitudes for a One Meter Amplitude Internal Wave Along Thermoclines at Various Depths

Thermocline Depth (m)	Density Difference (g/cc)	Wave Number (m^{-1})	Period T (sec)	Amplitude H_z Term (mv/100m/0.1 oe)
h' = 15	$\Delta\rho = 5\times10^{-3}$	0.01	7.88×10^{2}	0.0529
	$= 2\times10^{-3}$	0.01	1.25×10^{3}	0.0335
	$= 1\times10^{-3}$	0.01	1.76×10^{3}	0.0237
	$= 1\times10^{-4}$	0.01	5.57×10^{3}	0.0075
h' = 50	$\Delta\rho = 5\times10^{-3}$	0.01	5.04×10^{2}	0.0239
	$= 2\times10^{-3}$	0.01	7.98×10^{2}	0.0151
	$= 1\times10^{-3}$	0.01	1.13×10^{3}	0.0107
	$= 1\times10^{-4}$	0.01	3.57×10^{3}	0.0034
h' = 100	$\Delta\rho = 5\times10^{-3}$	0.01	4.32×10^{2}	0.0124
	$= 2\times10^{-3}$	0.01	6.82×10^{2}	0.0078
	$= 1\times10^{-3}$	0.01	9.65×10^{2}	0.0055
	$= 1\times10^{-4}$	0.01	3.05×10^{3}	0.0018
h' = 15	$\Delta\rho = 5\times10^{-3}$	0.1	1.30×10^{2}	0.0227
	$= 2\times10^{-3}$	0.1	2.06×10^{2}	0.0143
	$= 1\times10^{-3}$	0.1	2.91×10^{2}	0.0101
	$= 1\times10^{-4}$	0.1	9.21×10^{2}	0.0032
h' = 50	$\Delta\rho = 5\times10^{-3}$	0.1	1.27×10^{2}	0.0007
	$= 2\times10^{-3}$	0.1	2.01×10^{2}	0.0003
	$= 1\times10^{-3}$	0.1	2.84×10^{2}	0.0002
	$= 1\times10^{-4}$	0.1	8.97×10^{2}	0.0001
h' = 100	$\Delta\rho = 5\times10^{-3}$	0.1	1.27×10^{2}	0.0000
	$= 2\times10^{-3}$	0.1	2.01×10^{2}	0.0000
	$= 1\times10^{-3}$	0.1	2.84×10^{2}	0.0000
	$= 1\times10^{-4}$	0.1	8.97×10^{2}	0.0000

using the values: $g = 9.8062$ m/sec^2; the density ρ' of the upper layer was set equal to 1.0000; the electrode separation PQ was 100 m; the depth of the bottom h'' was taken to be 1500 m; and the values of the Earth's magnetic field intensity before conversion to units of $\underset{\sim}{B}$ were $H_x = H_z = 0.10$ oersted. The H_z contributions have been so evaluated as to afford a reference from which to obtain additional information. Multiples of amplitude or of the Earth's magnetic field intensity can easily be dealt with since their corresponding H_z signals can be found through direct multiplication. Double the amplitude or double the magnetic field and the H_z signal doubles.

Analysis

The H_x component of the GEK signal was found to be negligible for all the parametric values listed in Table 1. Examination of the calculations reveals that for thermocline depths less than 100 m, the H_z term dominates the signal completely. For depths exceeding 100 m, the H_x term begins to assert its influence. However, the rapid convergence of the signal to zero, due to the hyperbolic trigonometric functions, masks this resurgence of the H_x component.

The magnitude of the GEK signal (H_z term) is determined primarily by the local intensity of the vertical component of the Earth's magnetic field. The vertical magnetic field intensity, H_z, varies from 0.10 oersted near the equator to 0.50 oersted at mid

and high latitudes. Thus, the voltages listed for a one meter amplitude wave in Table 1 would be large enough ($\geq$ 0.1 mv) to be detectable in the mid and high latitudes. As one approaches the equator, the signals would approach zero. A second factor in determining the magnitude of the voltage is the wave amplitude. This direct proportionality between signal voltage and wave amplitude is, perhaps, of greatest importance at larger depths.

An overall examination of the GEK expression yields its intrinsic characteristics. For fixed latitude and wave number, the signal increases as the depth of the thermocline decreases. Similarly, for fixed latitude and thermocline depth, the signal increases as the wave number k decreases. Moreover, for values of $k \geq 1\ m^{-1}$, the properties of the inherent hyperbolic trigonometric functions cause the signal to become undetectable regardless of depth, latitude, or density difference. Finally, as the density difference across the thermocline increases, the GEK response will increase.

A summarization of these characteristics shows that the GEK theory of internal waves presented here is valid for interfacial waves in the range $k \geq 1 \times 10^{-4}\ m^{-1}$ to $k = 10\ m^{-1}$ (Appendix I). Below 100 m depth, the signal approaches zero for all wave numbers k. Waves with wave number $k \geq 1\ m^{-1}$ produce no detectable signal. Near the equator, signals for all wave numbers k, regardless of amplitude, approach zero. It is also important to note that other

factors existent in nature will significantly influence signal detectability. Appendix VI reviews such environmental effects and points out the experimental precautions that should be taken.

Finite Amplitude Internal Waves

GEK Theory

The electromagnetic theory presented at the beginning of this chapter put no restriction on the wave amplitudes for which it was valid. Therefore, as long as a stream function can be found for the finite amplitude interfacial wave motion, the GEK theory for internal waves will be applicable. The investigation will consider only finite amplitude waves of second-order. The stream functions and related velocity distributions will be determined as a prelude to the calculation of the finite amplitude GEK signatures.

Finite Internal Wave Literature Summary

Owing to the complexity of the equations of motion for finite amplitude interfacial waves, approximation techniques had to be developed to permit solution of even the simplest cases. Kotchine (1928) was the first to prove the existence of finite amplitude waves of permanent form at the interface of a two-layer system. His second-order approximation was limited, however, in its considering

only fluids of infinite depth. Solution of the finite depth case was not accomplished until Hunt (1961) extended the Stokes expansion technique to include a finite two-fluid system. His model, though, was bounded by horizontal rigid plates. The free surface, finite depth, and finite amplitude problem was solved only recently by Thorpe (1968).

Study of continuous density profile situations in relation to finite amplitude waves has been carried on simultaneously with the works mentioned above. Exact solutions for finite amplitude internal wave trains were first discussed by Long (1953). Yih (1960a) and Sen Gupta (1962) have expanded Long's single special case, wherein the equations of motion were linear, to include a family of similar cases. Peters and Stoker (1960), Long (1965), and Benjamin (1967) have developed approximation techniques for waves in continuously stratified fluids. These deal mostly with long solitary waves. An extension of the solitary wave approximations to finite amplitude wave trains can be found in Thorpe (1968). Thorpe (1968) also provides a thorough review of the history of finite amplitude wave theory.

Finite Amplitude Interfacial Wave Theory

The theoretical model and geometry to be used are identical to that shown in Figure 2. An infinitely long-crested finite amplitude wave is moving along the interface in the positive x-direction. We

will insist again that the fluid has a free surface, is incompressible:

$$\nabla \cdot \underset{\sim}{v} = 0 , \tag{2.35}$$

and is irrotational:

$$\nabla \times \underset{\sim}{v} = 0 . \tag{2.36}$$

The second-order equations of motion are found through an application of the Stokes expansion approximation as derived in Appendix II.

Thorpe (1968) solved these second-order equations of motion for the free surface and interfacial wave profiles. The associated velocity-potential functions[1/] he obtained for the two layers are:

$$\Phi' = -\frac{a\sigma}{rk}[\cosh k(z-h') + p \sinh k(z-h')] \sin(kx-\sigma t) +$$

$$+ [A_1 \cosh 2k(z-h') + A_2 \sinh 2k(z-h')] \sin 2(kx-\sigma t),$$

$$\Phi'' = \frac{a\sigma \cosh k(z+h'')}{k \sinh kh''} \sin(kx-\sigma t) + B \cosh 2k(z+h'') \sin 2(kx-\sigma t) \tag{2.37}$$

where $$B \sinh 2kh'' = A_1(2p \cosh 2kh' - \sinh 2kh') +$$

$$- \frac{a^2\sigma}{2}\left(\frac{s}{r} + \frac{1}{T_2}\right) - \frac{3a^2\sigma p}{4r^2}(1-p^2)\cosh 2kh',$$

and $$A_1 = \frac{a^2\sigma S_2}{\gamma \cosh 2kh'} \left\{ \frac{3p(1-p^2)}{2r^2 S_2} \cosh 2kh' [2p(\rho' S_1 S_2 + \rho'') - (\rho''-\rho')S_2] \right.$$

$$\left. + p\left[\frac{\rho''}{2}\left(\frac{1}{T_2^2} - 3\right) - \frac{\rho'}{2}\left(\frac{s^2}{r^2} - 3\right) + \frac{2\rho''}{S_2}\left(\frac{s}{r} + \frac{1}{T_2}\right)\right] - (\rho''-\rho')\frac{s}{r} \right\},$$

[1/] Personal communication from Dr. S. A. Thorpe, National Institute of Oceanography, Wormley, Surrey, England.

and

$$A_2 = 2pA_1 - \frac{3a^2\sigma p(1-p^2)}{4r^2},$$

$$p = \sigma^2/gk \quad , \qquad r = \sinh kh' - p\cosh kh' ,$$

$$s = \cosh kh' - p\sinh kh' ,$$

$$T_1 = \tanh kh' \quad , \qquad T_2 = \tanh kh'' ,$$

and

$$S_1 = \tanh 2kh', \qquad S_2 = \tanh 2kh'',$$

$$\gamma = 4p^2(\rho' S_1 S_2 + \rho'') - 2p\rho''(S_1 + S_2) + (\rho'' - \rho')S_1 S_2 ,$$

and the dispersion relation is, to second-order,

$$\sigma^4(\rho' T_1 T_2 + \rho'') - \sigma^2 gk\rho''(T_1 + T_2) + (\rho'' - \rho')T_1 T_2 (gk)^2 = 0. \quad (2.38)$$

There are additional linear time-dependent terms in each of the velocity-potential functions which are not shown in equation (2.37).

It is important to note that the validity of the Stokes expansion used here is maintained only if

$$\frac{aL}{h'^2} << 1 . \quad (2.39)$$

Long internal waves for which this condition does not hold must be solved according to another expansion technique. Thorpe (1968) is a good reference in this regard.

Also, these velocity-potentials were derived under the assumption that

$$\frac{\partial \Phi}{\partial x} = \frac{\partial \psi}{\partial z} = u \ , \qquad \frac{\partial \Phi}{\partial z} = - \frac{\partial \psi}{\partial x} = w . \tag{2.40}$$

Equation (2.40) is the negative of equation (2.12) used in Appendix II and the GEK theory derived previously. A change of sign in the velocity-potentials Φ will result if one converts from equation (2.40) to equation (2.12).

Using equation (2.12) and making the sign corrections in equation (2.37), we can find the stream functions and velocity components u, w for each layer.

GEK Response and Analysis

The stream function ψ' can now be substituted into equations (2.19) and (2.21) to obtain the GEK signature. This will not be done here due to the complexity of the velocity-potentials of equation (2.37). Instead, the general nature of the GEK signature will be ascertained from knowledge of the wave forms and velocity-potentials.

As the density difference across the thermocline tends to zero, the free surface displacement tends to zero. This causes the free surface solutions to assume the form of the solutions found when the upper boundary is assumed rigid. A sufficient condition for the motion of the free surface to be neglected is (Thorpe, 1968):

$$\cosh kh' >> (\rho'' - \rho') T_1 / \rho''(T_1 + T_2) . \qquad (2.41)$$

Thus, when this relation is satisfied, the GEK signals due to interfacial waves in a free surface system will be identical to those generated by similar waves in a fluid model that has a fixed horizontal upper boundary. The difficulties encountered in working with a free surface can thereby be side-tracked by switching to a rigid upper boundary model. Moreover, this change of boundary conditions does not affect the validity of the resulting GEK signatures.

The case of interest is when h'' is large as compared to h', which corresponds to a shallow thermocline. If the density difference is small, the GEK signal will exhibit a departure from the sinusoidal due to the influence of second-order terms in the velocity-potentials. The signature will be one in which the troughs are narrower than the crests (or vice versa depending on your electrical grounding regime). As the thermocline depth increases, the signal will begin to appear symmetrical again. Sinusoidal symmetry will be reached when the interface is located exactly half way between the surface and the ocean bottom. Third-order effects, which we have not considered, should produce some flattening at both the crests and the troughs.

Recall, these GEK characteristics pertain to interfacial waves which are assumed to have a negligible surface displacement. The dispersion relation for such waves corresponds to that for finite

amplitude internal waves in an horizontally bounded upper surface model:

$$\sigma^2 = \frac{gk(\rho''-\rho')T_1T_2}{\rho'T_2+\rho''T_1}\left\{1+\frac{(ak)^2}{8T_1}(9-22T_1+13T_1^2+4T_1^3)\right\} \qquad (2.42)$$

If the surface effect is not negligible, which is rare in the natural ocean, the internal wave GEK signatures would have an additional surface GEK signal superimposed upon them. The final signal would be a combination of the two. The second-order effects from the internal component would probably be lost due to this superposition.

All of the small amplitude interfacial wave GEK characteristics, such as increased voltages at mid and high latitudes, still hold true here. The increased wave amplitude will, at most, simply protract the ranges of signal detectability.

CHAPTER III

GEK RESPONSE TO INTERNAL WAVES IN A CONTINUOUSLY STRATIFIED FLUID

Introduction

The GEK response to short internal waves in a continuously stratified fluid is presented to second-order. The wave model is assumed to be horizontally bounded at the upper surface thereby restricting the discussion to the internal wave modes. The general GEK theory is then applied to the specific example of internal waves of the lowest mode in a linear density profile. The towed electrode GEK signatures are evaluated through the identification of the velocity distribution and related stream functions.

GEK Theory

The development of the GEK theory for interfacial waves in Chapter II was influenced in part by the theoretical wave model in which the internal waves were to exist. Here again, the wave model will be significant in setting up the appropriate electromagnetic field equations. We shall assume at the outset that the model is bounded by a rigid horizontal plate at the upper surface. This assumption is of no consequence in determining the electromagnetic theory but does

eventually affect the form of the GEK signatures. A rigid upper boundary requires that the surface displacement be negligible. Thus, the GEK signature is the product of the field induced solely by the internal wave component of the wave motion. The absence of the surface component of the motion is not uncommon; yet, surface slick patterns from internal waves are observed occasionally. In cases wherein a rigid surface assumption is invalid, the GEK theory will remain the same, but the GEK signatures will be a composite of the surface and internal GEK signals as discussed in the finite amplitude section of Chapter II.

Consider a laterally unbounded deep ocean of depth H capped at the surface and at the bottom by rigid horizontal plates. The water in this sea will be assumed to be stably stratified producing a continuous density profile with depth. The sea floor will be assumed to possess the electrical conductivity of an insulator. The origin of the axes will lie on the sea floor at $z = 0$ with z being positive upward. The internal waves existent in this model will be infinitely long-crested in the y-direction and travelling in the positive x-direction. The velocity of the motion will be small compared to the speed of light allowing us to neglect free charges and displacement currents. The motion in the system will be due solely to internal waves of the lowest mode as shown in Figure 3. The external magnetic field is to be steady and uniform.

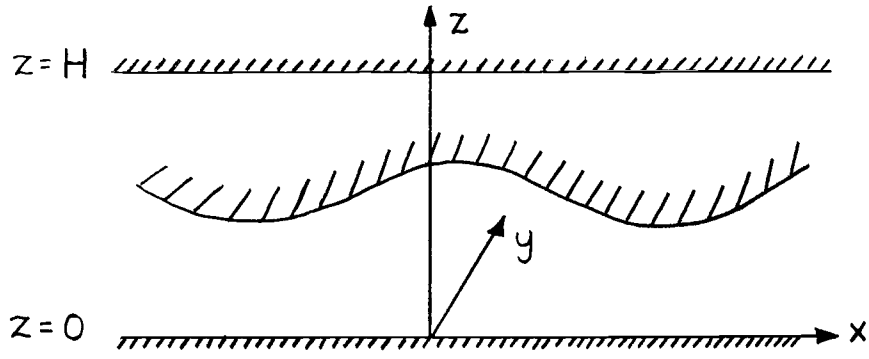

Figure 3. Continuous density internal wave geometry.

At this point we can revert back to the GEK theory of Chapter II. It will be applicable here with the following modifications. Equations (2.1) through (2.10) are valid as written provided we consider the ocean to consist of one as opposed to two layers. Equations (2.11) through (2.16) must have sign corrections made so that they conform with statements in equation (2.40). The results of equations (2.17) through (2.20) then convert to:

$$\phi = H_y \psi \,, \tag{3.1}$$

$$\rho \underset{\sim}{i} = (0, -H_x \frac{\partial \psi}{\partial x} - H_z \frac{\partial \psi}{\partial z}, 0) \,. \tag{3.2}$$

and the towed electrode GEK signal as defined by equation (2.21) becomes:

$$\text{GEK Signal} = \int_P^Q \rho \underset{\sim}{i} \cdot \underset{\sim}{d\ell} = \rho i \, PQ \Big|_{z=H} \tag{3.3}$$

where the notation follows that of Chapter II. Specific GEK signatures can now be derived by first determining the associated velocity distributions.

Internal Waves in Continuously Stratified Fluid

The investigation of internal waves in continuously stratified media was begun by Burnside (1889). He applied a limiting process to a multi-layered fluid to obtain the internal wave solutions for an exponential density profile. This work was reaffirmed by Love (1891) when he found an analytic solution for the same profile directly from the equations of motion. The general density profile was first discussed by Fjeldstadt (1933). His work set forth the standard Sturm-Liouville equation approach used most generally today. Subsequent work on internal waves in continuously stratified fluids then began to diversify into specific areas of interest. Solitary waves, finite amplitude progressive waves, and standing internal waves were all investigated separately. Since their history parallels that of interfacial wave theory, it has been reviewed in prior sections and will not be repeated here.

The method to be used in the wave theory to follow was developed by Thorpe (1966). It is one of repeated approximation similar to the expansion method developed by Stokes (1847). Since complete details can be found in Thorpe (1968), only the more pertinent aspects will

be presented.

Internal Wave Theory

Using the wave model shown in Figure 3, we will assume that the infinite train of internal gravity waves to be considered shall exist at all times in a stable fluid density structure. In addition, the fluid motion is to be limited to that which results from the presence of the waves. To insure the stability of this type of fluid motion, the associated Richardson number, R_i, must be everywhere greater than 1/4 (see Appendix III). This condition satisfies the stability demands but restricts the maximum amplitude the waves can possess. Any wave amplitude which exceeds the upper limit dictated by R_i can be expected to break and thereby fall out of the scope of consideration.

The upper surface of the model is to be bounded by a rigid plate. Neglecting the free surface displacements can be justified only by examining the particular density profile of interest. For the linear density profile to be investigated later, the free surface can be neglected provided first that the density difference between the top and bottom of the fluid is small and second that the terms usually neglected in the equations of motion when the Boussinesq approximation is made are indeed negligible (see Appendix IV). It is thought that in a general stratification under similar conditions the free surface motion may be neglected. This, however, has not been proven

(Thorpe, 1968).

Suppose that the fluid is incompressible (equation (2.23)) and the stream function ψ is defined in relation to the velocity components according to equation (2.40). The equation of vorticity then is written as:

$$\rho\left[\frac{\partial}{\partial t}\nabla^2\psi + J(\nabla^2\psi, \psi)\right] + \frac{\partial \rho}{\partial z}\left[\frac{\partial^2\psi}{\partial t \partial z} + J\left(\frac{\partial \psi}{\partial z}, \psi\right)\right] +$$

$$\frac{\partial \rho}{\partial x}\left[\frac{\partial^2\psi}{\partial t \partial x} + J\left(\frac{\partial \psi}{\partial x}, \psi\right)\right] = g\frac{\partial \rho}{\partial x} \qquad (3.4)$$

where J is the Jacobian with respect to x and z; ρ = density of the fluid; and the continuity equation is

$$\frac{\partial \rho}{\partial t} + J(\rho, \psi) = 0. \qquad (3.5)$$

The initial stable density distribution, $\rho_0(z)$, before the motion is generated is to be continuous and to have continuous first and second derivatives. The boundary conditions on ψ are that

$$\frac{\partial \psi}{\partial x} = 0 \qquad \text{at } z = 0, H. \qquad (3.6)$$

Applying the Boussinesq approximation (see Appendix IV), equation (3.4) reduces to:

$$\rho_0(0)\left[\frac{\partial}{\partial t}\nabla^2\psi + J(\nabla^2\psi, \psi)\right] = g\frac{\partial \rho}{\partial x}. \qquad (3.7)$$

Expand the stream function and the density in the following manner:

$$\psi = \sum_{n=1}^{\infty} \alpha^n \psi_n , \tag{3.8}$$

$$\rho = \sum_{n=1}^{\infty} \alpha^n \rho_n \tag{3.9}$$

where α is a small ordering parameter proportional to the wave amplitude. It can be shown that for a small enough α, the series will converge.

Differentiating (3.7) with respect to time and substituting $\partial\rho/\partial t$ from equation (3.5), we obtain:

$$\rho_0(0)\left[\frac{\partial^2}{\partial t^2}\nabla^2\psi + \frac{\partial}{\partial t} J(\nabla^2\psi, \psi)\right] = -g \frac{\partial}{\partial x} J(\rho, \psi) . \tag{3.10}$$

The First-order Solution

Substituting equation (3.8) for ψ and equation (3.9) for ρ into equation (3.10) and equating coefficients of α yields:

$$\frac{\partial^2}{\partial t^2}\nabla^2\psi_1 = \frac{g}{\rho_0(0)} \frac{d\rho_0}{dz} \frac{\partial^2\psi_1}{\partial x^2} . \tag{3.11}$$

A progressive wave solution of equation (3.11) and the boundary conditions (3.6) is:

$$\psi_1 = \Psi(z)\cos(kx - \sigma t) \tag{3.12}$$

where Ψ is one of the eigenfunctions $\{\Psi_n\}$ of

$$\Psi'' - k^2\Psi - \frac{g}{\rho_0(0)} \frac{d\rho_0}{dz} \frac{1}{c^2} \Psi = 0 \qquad (3.13)$$

wherein the primed symbols denote the power of the derivatives with respect to z; and $c = \sigma/k$. The value of c is the first term in the series expansion:

$$c = \sum_{n=1}^{\infty} \alpha^n c^{(0)} . \qquad (3.14)$$

The $c^{(1)}$, $c^{(2)}$, $\cdots$, $c^{(n)}$ terms will be found by equating coefficients if terms of the form $(d\rho_0/dz)\,\Psi\cos(kx - \sigma t)$ appear on the right-hand side of equation (3.10) when expansions to order α^2, α^3, $\cdots$ are made.

There are two sets of eigenfunctions which will satisfy equation (3.13). Both are complete and orthogonal. One set for fixed k^2 has a corresponding set of eigenvalues $\{c_n^2\}$. The other set for fixed c^2 has a corresponding set of eigenvalues $\{k_n^2\}$. Therefore, we may consider the problem by specifying either a wave number or a fixed phase speed. It is important to note that each set of eigenfunctions possesses inherent characteristics which may make it more useful than the other in specific problems. Details in this regard are found in Thorpe (1968), Yih (1960a), and Yanowitch (1962).

Second-order Solution

By equating coefficients of α^2 in equation (3.10) and substituting the known solutions for ψ_1 and the related ρ_1, we can obtain the governing equations of motion to second-order:

$$\frac{\partial^2}{\partial t^2} \nabla^2 \psi_2 - \frac{g}{\rho_0(0)} \frac{d\rho_0}{dz} \frac{\partial^2 \psi_2}{\partial x^2} = \frac{2\Psi^2}{\rho_0(0)} \frac{d^2\rho_0}{dz^2} \frac{gk^3}{\sigma} \cos 2(kx - \sigma t). \quad (3.15)$$

with boundary conditions:

$$\frac{\partial \psi_2}{\partial x} = 0 \qquad \text{at } z = 0, H. \quad (3.16)$$

We will stop the derivation here to consider the linear density profile example. Moreover, the remainder of the general density second-order solution technique will be omitted since it will not be needed for this particular case. However, the continuation of the derivation in most density situations will be necessary and can be found in Thorpe (1968).

Linear Density Profile

Consider periodic finite amplitude internal waves in a fluid of linear density profile:

$$\rho_0 = \rho_0(0)(1 - \mu z) \quad (3.17)$$

bounded by horizontal planes at $z = 0, H$. For this case, equation

(3.15) reduces to equation (3.11) since the second derivative of the initial density vanishes. Therefore, we can define $\psi_2 = 0$ and the solution ψ_1 of equation (3.11) will be valid to second-order. The second-order density, ρ_2, is not necessarily zero, however, nor can the second-order effects on the wave profile be ignored.

The eigenfunction equation (3.13) becomes:

$$\Psi'' - (k^2 - \frac{g\mu}{c^2})\Psi = 0 \tag{3.18}$$

which has solutions, which satisfy the boundary conditions, of the form:

$$\Psi = \sin(n\pi z/H) \tag{3.19}$$

where n is an integer corresponding to the mode of the wave. The equation for the wave number is:

$$(\frac{n\pi}{H})^2 = k^2(\frac{g\mu}{\sigma^2} - 1) . \tag{3.20}$$

To second-order, the stream function is:

$$\psi = \alpha \sin(n\pi/H)\cos(kx - \sigma t). \tag{3.21}$$

For the expansion procedure to be valid, Thorpe (1968) shows that the parameter α must be

$$\frac{\alpha k}{\sigma}\frac{n\pi}{4H} << 1 \tag{3.22}$$

where

$$a = (\alpha k/\sigma) = \text{wave amplitude at height } z = H/2 . \qquad (3.23)$$

In other words, since H/n is the vertical scale of the motion, the wave amplitude must be small in comparison to the vertical scale of the motion. Likewise, if μH is small, meaning that the fractional density difference is small, the free surface motion may be neglected. If μH is not small, a free surface displacement appears which is out of phase with the internal oscillation.

GEK Signature Analysis

The second-order stream function equation (3.21) can now be substituted into equations (3.2) and (3.3) to obtain the towed electrode GEK signature. For the lowest mode ($n = 1$), we get

$$\text{GEK Signal} = H_z \ell . \frac{\sigma a \pi}{kH} \cos (kx - \sigma t) \qquad (3.24)$$

where σ is determined from equation (3.20).

Numerical computations for a linear density profile wave reveal that its GEK responses for $k = 0.01\ m^{-1}$ and $k = 0.001\ m^{-1}$ are 0.002 mv and 0.009 mv respectively for: one meter wave amplitude, $H_z = 0.01$ oersted; $g = 9.8062\ m/sec^2$; $\mu = 1 \times 10^{-5}\ m^{-1}$; and $H = 1500$ m. It should be noted that the small values of wave amplitude and H_z were again chosen to facilitate multiplication. Signal magnitudes for higher wave amplitudes or higher H_z values

can be obtained by direct multiplication of the voltages listed.

Examination of equation (3.24) will yield the general characteristics of the GEK signature. Like interfacial waves, the response at a fixed location decreases as the wave number increases. Similarly, for a fixed location and fixed wave number, the signal increases as the density gradient increases. The latitudinal response due to changes in the Earth's magnetic field intensity, H_z, and the direct proportionality of signal magnitude to wave amplitude are the same as that of interfacial waves. Peculiar to the linear density case, however, is the trend of signal decrease as the total depth H increases.

The signal magnitudes for continuous stratification internal waves as compared to interfacial waves are smaller for identical environmental parameters. This is due primarily to the fact that the particle velocities in continuous systems are significantly smaller. The ultimate responsibility, though, can be traced to the density gradients. Continuous density internal waves will exist in systems with gradients of the order of 1×10^{-5} g/cc/m while interfacial oscillations exist along gradients which are one to two orders of magnitude larger. The larger gradient produces larger particle velocities which generate larger signal voltages.

An overall view of these characteristics suggests that for wave numbers $k \geq 0.1\ m^{-1}$ the signal will be undetectable within the

limitations set by the theory and by nature. Waves with smaller values of k will be detectable especially in the higher latitudes. The natural effects of the local environment (see Appendix IV) and the possible influence of a free surface displacement must always be taken into account when evaluating observed GEK signatures.

Finally, this analysis applies to finite but small internal waves under the assumption that the effects of turbulence are negligible. In general, however, turbulence must be considered when dealing with other than small amplitude internal waves.

CHAPTER IV

GEK RESPONSE TO STANDING INTERNAL WAVES

Internal standing waves are a segment of the wave structure of continuous density systems which warrant special consideration. Their very nature sets them in a class apart from progressive waves and requires that their GEK signatures be pursued separately.

Since most internal wave phenomena are of a magnitude such that they do not disturb the ocean surface, we will consider only the GEK effects of the internal component of the standing wave pattern. Let us assume that the waves are of the lowest mode and exist in a system described by the model of Figure 3. We will ignore the ocean currents that usually set up this type of internal wave and will concentrate only on the motion due to the waves themselves. Without being rigorous, it can be shown that the stream function for a sinusoidal standing wave in the given model is of the form:

$$\psi = F \sin(\pi z/H) \sin kx \cos \sigma t \tag{4.1}$$

where F is a function of the wave amplitude, density gradient, gravitational acceleration, and angular frequency as determined by the boundary conditions of the particular problem. Thus, the u component of the particle velocity according to equation (2.40) will be:

$$u = \frac{\partial \psi}{\partial z} = \frac{\pi}{H} F \cos\left(\frac{\pi z}{H}\right) \sin kx \cos \sigma t . \qquad (4.2)$$

Equation (4.2) states that at a fixed location the horizontal particle velocity is zero as is expected for standing waves. Likewise, at the horizontally bounded surface where the signal is measured, the w component of velocity is assumed zero. Therefore, electrodes towed in the usual manner, at the surface perpendicular to the direction of propagation, will record no signal due to the internal standing wave. If the sea surface is assumed free, the w particle velocity will no longer be zero and the H_x term of equation (3.2) will induce a GEK signature. However, the magnitude of the voltage will be negligible since the surface displacements are typically of the order of centimeters or less.

Thus, from this discussion, it is reasonable to conclude that in nature the GEK response to internal standing waves is undetectable. Moreover, most internal standing waves will generate no GEK signal at all.

BIBLIOGRAPHY

Barber, N. F. 1948. The magnetic field produced by Earth currents flowing in an estuary or sea channel. Monthly Notices of the Royal Astronomical Society 5(7):258-269.

Barber, N. F. and M. S. Longuet-Higgins. 1948. Water movements and Earth currents: electrical and magnetic effects. Nature 161:192-193.

Benjamin, T. B. 1966. Internal waves of finite amplitude and permanent form. Journal of Fluid Mechanics 25(2):241-270.

Benjamin, T. B. 1967. Internal waves of permanent form in fluids of great depth. Journal of Fluid Mechanics 29(3):559-592.

Bogdanov, M. A. and I. A. Ivanov. 1960. Toki v more i izmerenie techenii pribrom EMIT. [Electric currents at sea and current measurements by electromagnetic current meters.] Akademiia Nauk SSSR. Institut Okeanologii, Trudy 39:80-84.

Bowden, K. F. 1953. Measurement of wind currents in the sea by the method of towed electrodes. Nature 171(2):735-737.

Bowden, K. F. 1956. The flow of water through the Straits of Dover, related to wind and differences in sea level. Philosophical Transactions of the Royal Society (London), Series A. 248: 517-551.

Bowden, K. F. and P. Hughes. 1961. The flow of water through the Irish Sea and its relation to wind. The Geophysical Journal of the Royal Astronomical Society 5(4):265-291.

Burnside, W. 1889. On the small wave-motions of a heterogeneous fluid under gravity. London Mathematical Society, Proceedings 20:392-397.

Chew, F. 1958. An interpretation of the transverse component of the Geomagnetic Electrokinetograph readings in the Florida Straits off Miami. American Geophysical Union, Transactions 39(5):875-884.

Chew, F. 1967. On the cross-stream variation of the k-factor for geomagnetic electrokinetograph data from the Florida current off Miami. Limnology and Oceanography 12(1):73-78.

Defant, A. 1950. On the origin of internal tide waves in the open sea. Journal of Marine Research 9(2):111-119.

Defant, A. 1961. Physical oceanography. New York, Macmillan. 2 vols.

Drazin, P.G. and L.N. Howard. 1966. Hydrodynamics stability of parallel flow of inviscid fluid. Advances in Applied Mechanics 9:1-89.

Faraday, M. 1832. The Bakerian lecture - experimental researches in electricity. Philosophical Transactions of the Royal Society (London), part 1, p. 163-177.

Fjeldstadt, J.E. 1933. Interne Wellen. Geofysiske Publikasjoner 10(6):1-35.

Fonarev, G.A. 1961a. Marine telluric currents and their relationship to magnetic variations. Geomagnetism and Aeronomy 1(1):77-80.

Fonarev, G.A. 1961b. Variations in marine telluric currents. Geomagnetism and Aeronomy 1(3):374-377.

Fonarev, G.A. 1961c. Some data on telluric currents in the Barents Sea. Geomagnetism and Aeronomy 1(4):530-535.

Fonarev, G.A. 1963. Vertical electric currents in the sea. Geomagnetism and Aeronomy 3(4):636-637.

Fonarev, G.A. 1964. Distribution of electromagnetic variations with depth in the sea. Geomagnetism and Aeronomy 4:881-882.

Fonarev, G.A. 1968. The effect of ocean telluric currents on the operation of the GEK current meter. Oceanology 8(4):579-585.

Fonarev, G.A. and V.V. Novysh. 1965. Some results of telluric current measurements at station North Pole-10 in 1963. Academy of Sciences of the USSR, Doklady, Earth Science Section 160(2):1-2.

Fobush, S.E. and M. Casaverde. 1961. Equatorial electrojet in Peru. Carnegie Institution of Washington. Washington, D.C. Publication 620. 135 p.

Glasko, V.B. and A.G. Sveshnikov. 1961. On electric fields in ocean currents caused by the Earth's magnetic field. Geomagnetism and Aeronomy 1:68-75.

Gorodnicheva, O.P. 1966. Current measurements by electromagnetic current meter in the Gulf Stream area. Oceanology 6(3):418-425.

Greenhill, A.G. 1887. Wave motion in hydrodynamics. American Journal of Mathematics 9:62-112.

Haurwitz, B. 1950. Internal waves of tidal character. American Geophysical Union. Transactions 31:47-52.

Heyna, B. and P. Groen. 1958. On short-period internal gravity waves. Physica 24:383-389.

Howard, L.N. 1961. Note on a paper of John W. Miles. Journal of Fluid Mechanics 10(4):509-512.

Hughes, P. 1962. Towed electrodes in shallow water. The Geophysical Journal of the Royal Astronomical Society 7:111-124.

Hunt, J.N. 1961. Interfacial waves of finite amplitude. La Houille Blanche 4:515-531.

Ivanov, V.I. and D.P. Kostomarov. 1963. Computation of electric currents induced in the sea by S_q variations. Geomagnetism and Aeronomy 3(6):868-875.

Knauss, J.A. and J.L. Reid. 1957. The effects of cable design on the accuracy of the GEK. American Geophysical Union. Transactions 38:320-325.

Kolin, A. 1944. Electromagnetic velometry. I. A method for the determination of fluid velocity distribution in space and time. Journal of Applied Physics 15(2):150-164.

Konaga, S. 1964. On the current velocity measured with geomagnetic electrokinetograph. Journal of the Oceanographical Society of Japan 20(1):1-6.

Kotchine, N. 1928. Determination Rigoureuse des Ondes Permanentes d'Ampleur Finie a la Surface de Separation de Deux Liquides de Profondeur Finie. Mathematische Annalen 98:582-615.

Krauss, W. 1961. Zur Trochoidenahnlichen Form der Kurzen Fortschreitender Internen Grenzflachenwellen. Keiler Meeresforschungen 17:159-162.

Krauss, W. 1964. Interne Wellen in einem exponentiell geschichteten Meer. Kieler Meeresforschungen 20(2):109-123.

LaFond, E.C. 1962. Internal waves. In: The sea, ed. by M.N. Hill. Vol. 1. New York, Interscience. p. 731-751.

Lamb, H. 1945. Hydrodynamics. 6th ed. New York, Dover. 738 p.

Larsen, J.C. 1966. Electric and magnetic fields induced by oceanic tidal motion. Ph.D. thesis. La Jolla, University of California at San Diego. 99 numb. leaves.

Larsen, J.C. and C. Cox. 1966. Lunar and solar daily variation in the magnetotelluric field beneath the ocean. Journal of Geophysical Research 71(18):4441-4445.

Lee, O.S. 1965. Internal waves in the sea: a summary of published information with notes on applications to naval operations. U.S. Navy Electronics Lab. San Diego, California. NEL Report 1302. 58 p.

Long, R.R. 1953. Some aspects of the flow of stratified fluids. I. A theoretical investigation. Tellus; a Quarterly Journal of Geophysics 5:42-58.

Long, R.R. 1965. On the Boussinesq approximation and its role in the theory of internal waves. Tellus; a Quarterly Journal of Geophysics 17(1):46-52.

Longuet-Higgins, M.S. 1947. The electric field induced in a channel of moving water. Admiralty Research Laboratory. Teddington, Eng. 21 numb. leaves. Report ARL/R.2/102.22/W.

Longuet-Higgins, M.S. 1949. The electrical and magnetic effects of tidal streams. Monthly Notices of the Royal Astronomical Society. Geophysical Supplement 5(8):297-307.

Longuet-Higgins, M.S., M.E. Stern and H. Stommel. 1954. The electrical field induced by ocean currents and waves, with applications to the method of towed electrodes. Woods Hole, Massachusetts. 37p. (Woods Hole Oceanographic Institution. Papers in Physical Oceanography and Meteorology, Vol. 8. no. 1)

Love, A.E.H. 1891. Wave motion in a heterogeneous heavy liquid. London Mathematical Society. Proceedings 22:307-316.

Magaard, L. 1965. Zur Theorie zweidimensionaler nichtlinearer interner Wellen in stetig geschichteten Medien. Kieler Meeresforschungen 21(1):22-32.

Malkus, W.V.R. and M.E. Stern. 1952. Determination of ocean transports and velocities by electromagnetic effects. Journal of Marine Research 11:97-105.

Mangelsdorf, P.C., Jr. 1962. The world's longest salt bridge. Marine Sciences Instrumentation. Vol. 1. New York, Plenum Press. p. 173-185.

Moroshkin, K.V. 1957. Opyty raboty s electromagnitnym izmeritelem techenii v otkrytom. [Experimental operation of an electro-magnetic current meter in the open sea.] Akademiia Nauk SSSR. Institut Okeanologii, Trudy 25:62-87.

Morse, R.M., M. Rattray, Jr., R.G. Paquetle and C.A. Barnes. 1958. The measurement of transports and currents in small tidal streams by an electromagnetic method. Seattle, Washington. 70 numb. leaves. University of Washington. Dept. of Oceanography. Technical Report no. 57.

Novysh, V.V. 1965. Accuracy in determination of the vertical component of the geomagnetic field by geomagnetic current meter. Oceanology 5(4):110-115.

Novysh, V.V. and G.A. Fonarev. 1963. Telluric currents in the Arctic Ocean. Geomagnetism and Aeronomy 3:919-921.

Novysh, V.V. and G.A. Fonarev. 1966. Some results of electromagnetic investigations in the Arctic Ocean. Geomagnetism and Aeronomy 6(2):325-327.

Peters, A.S. and J.J. Stoker. 1960. Solitary waves in liquids having non-constant density. Communications on Pure and Applied Mathematics 13(1):115-164.

Phillips, O.M. 1966. The dynamics of the upper ocean. Cambridge, Cambridge University. 261 p.

Rattray, M., Jr. 1957. Propagation and dissipation of long internal waves. American Geophysical Union. Transactions 38:495-500.

Reid, J.L., Jr. 1958. A comparison of drogue and GEK measurements in deep water. Limnology and Oceanography 3(2):160-165.

Richardson, W.S. and W.J. Schmitz, Jr. 1965. A technique for the direct measurement of transport with application to the Straits of Florida. Journal of Marine Research 23(2):172-185.

Runcorn, S. 1964. Measurements of planetary electric currents. Nature 202:10-13.

Sanford, T.B. 1967. Measurement and interpretation of motional electric fields in the sea. Ph.D. thesis, Cambridge, Massachusetts Institute of Technology. 161 numb. leaves.

Sen-Gupta, B.K. 1962. Large-amplitude periodic lee waves in stratified fluids, Part II, Linear solution. Royal Meteorological Society. Quarterly Journal 88:426-429.

Solov'yev, L.G. 1961. Measurement of electric fields in the sea. Academy of Sciences of the USSR Doklady, Earth Science Section 138(2):32-34.

Spiegel, E.A. and G. Veronis. 1960. On the Boussinesq approximation for a compressible fluid. Astrophysical Journal 131(2):442-447.

Stokes, G.G. 1847. On the theory of oscillatory waves. Cambridge Philosophical Society. Transactions 8:441-455.

Stommel, H. 1948. The theory of the electric field induced in deep ocean currents. Journal of Marine Research 7:386-392.

Sysoev, N.N. and V.G. Volkov. 1957. Rukovodstvo po elektromagnitnomu metodu izmereniia skorosti morskikh techenii na khodu sudna. [Manual of the techniques of electromagnetic measurement of ocean-current velocities under way.] Akademiia Nauk SSSR. Institut Okeanologii, Trudy 24:173-199.

Thorpe, S.A. 1966. On wave interactions in a stratified fluid. Journal of Fluid Mechanics 24(4):737-751.

Thorpe, S.A. 1968. On the shape of progressive internal waves. Philosophical Transactions of the Royal Society of London. Series A. 263:563-614.

Tikhonov, A.N. and A.G. Sveshnikov. 1959. On the slow motion of conducting medium in a stationary magnetic field. Bulletin, Academy of Sciences of the USSR, Geophysics Series 1:30-34.

Vaux, D. 1955. Current measuring in shallow waters by towed electrodes. Journal of Marine Research 14:187-194.

von Arx, W.S. 1950. An electromagnetic method for measuring the velocities of ocean currents from a ship under way. Woods Hole, Massachusetts. 62 p. (Woods Hole Oceanographic Institution. Papers in Physical Oceanography and Meteorology. Vol. 11. no. 3)

von Arx, W.S. 1952. Notes on the surface velocity profile and horizontal shear across the width of the Gulf Stream. Tellus; a Quarterly Journal of Geophysics 4(3):211-214.

Wertheim, G.K. 1954. Studies of the electrical potential between Key West, Florida, and Havana, Cuba. American Geophysical Union. Transactions 35(6):872-882.

Williams, E.J. 1930. The induction of electromotive forces in a moving liquid by a magnetic field, and its application to an investigation of the flow of liquids. Physical Society of London. Proceedings 42:466-487.

Yanowitch, M. 1962. Gravity waves in a heterogeneous incompressible fluid. Communications on Pure and Applied Mathematics 15(1):45-61.

Yih, C-S. 1960a. Gravity waves in a stratified fluid. Journal of Fluid Mechanics 8(4):481-508.

Yih, C-S. 1960b. Exact solutions for steady two-dimensional flow of a stratified fluid. Journal of Fluid Mechanics 9(2):161-174.

Young, F.B., H. Gerrard and W. Jevons. 1920. On electrical disturbances due to tides and waves. The Philosophical Magazine and Journal of Science. Sixth Series 40:149-159.

APPENDICES

APPENDIX I

INDUCED MAGNETIC VARIATIONS

Oscillating electric currents, such as those induced by wave motion, generate associated magnetic field fluctuations. These magnetic field fluctuations in turn induce a secondary electric current which may affect the original electron flow. This relationship is described according to Maxwell's equations in terms of the electric field intensity. It is written as

$$\underset{\sim}{E} = - \nabla\phi - \frac{\partial \underset{\sim}{A}}{\partial t} \qquad (A.1.1)$$

where ϕ is the electrostatic scalar potential and $\underset{\sim}{A}$ is the magnetic vector potential.

Sanford (1967) demonstrates that, for magnetic field variations induced by wave motion with wave number k, $\frac{\partial \underset{\sim}{A}}{\partial t}$ and the associated induced electric currents are negligible if

$$k\delta > \sqrt{2} \qquad (A.1.2)$$

where δ is the skin depth for electromagnetic wave penetration.

This condition is derived by considering Ohm's Law for a medium moving with velocity $\underset{\sim}{v}$ in a magnetic field.

$$\underset{\sim}{J} = \sigma [\underset{\sim}{E} + \underset{\sim}{v} \times \underset{\sim}{B}] \qquad (A.1.3)$$

Neglecting free charges and displacement currents, we apply two of Maxwell's equations

$$\nabla \times \underset{\sim}{E} = - \frac{\partial \underset{\sim}{B}}{\partial t} , \qquad (A.1.4)$$

$$\nabla \times \underset{\sim}{B} = \mu \underset{\sim}{J} \qquad (A.1.5)$$

to equation (A.1.3) and obtain

$$\frac{\partial \underset{\sim}{B}}{\partial t} = \nabla \times \underset{\sim}{v} \times \underset{\sim}{B} + \frac{1}{\mu\sigma} \nabla^2 \underset{\sim}{B} . \qquad (A.1.6)$$

Let $\underset{\sim}{B} = \underset{\sim}{F} + \underset{\sim}{B}'$ where $\underset{\sim}{F}$ is the steady, uniform geomagnetic field and $\underset{\sim}{B}'$ the magnetic variation. In addition, let us assume that $\underset{\sim}{v}$ and $\underset{\sim}{B}'$ are of the form

$$\underset{\sim}{v} = \underset{\sim}{v}_0 \exp[i(\underset{\sim}{k} \cdot \underset{\sim}{x} - \omega t)] , \qquad (A.1.7)$$

$$\underset{\sim}{B}' = \underset{\sim}{B}'_0 \exp[i(\underset{\sim}{k}' \cdot \underset{\sim}{x} - \omega t)] . \qquad (A.1.8)$$

Then equation (A.1.6) states approximately that

$$c\left(1 - \frac{v_0}{c} + \frac{ik'^2}{\mu\sigma\omega}\right) B'_0 = - F_0 v_0 \qquad (A.1.9)$$

where $c = \omega/k$. Since $v_0/c << 1$, we can neglect the time variations in the magnetic field provided:

$$\left| \frac{ik'^2}{\mu\sigma\omega} \right| > 1 . \qquad (A.1.10)$$

The wave number k' is complex but its modulus should be of order k.

By definition $\mu\sigma\omega = 2/\delta^2$ where δ is the skin depth for electromagnetic wave penetration in a conducting medium. Equation (A.1.10) then reduces to

$$k\delta > \sqrt{2} . \qquad \text{(A.1.2)}$$

Examination of this relation reveals that $\frac{\partial \underline{\underline{A}}}{\partial t}$ can be neglected for surface waves which fall within the wave number range $k = 10\,m^{-1}$ to $k = 10^{-3}\,m^{-1}$. Similarly, $\frac{\partial \underline{\underline{A}}}{\partial t}$ and the associated induced secondary electric currents are negligible for internal waves within the wave number range $k = 10\,m^{-1}$ to $k = 10^{-4}\,m^{-1}$ at depths below five meters.

It is noteworthy that long-period surface waves such as tsunamis (see Appendix V) in general are not within the wave number range for which $\frac{\partial \underline{\underline{A}}}{\partial t}$ and the related electric currents are negligible. However, from consideration of Lenz's Law it would appear that the induced secondary currents would act in such a way as to reduce rather than enhance the primary wave-induced electric current. The result would be that the invalid application of the GEK theory herein discussed would yield GEK signals larger than should be expected.

APPENDIX II

SECOND-ORDER PROGRESSIVE INTERFACIAL WAVE THEORY

In dealing with finite amplitude waves, it is necessary to re-examine the equations of motion of a wave system and to reevaluate the various terms omitted under the assumptions of infinitesimal wave amplitude. This is especially true in cases where the fluid surface is free and unbounded. After the omitted terms have been properly reinstated, it is necessary to solve these revised equations of motion for wave modes of finite amplitude. Typically, however, there exists few such exact solutions so that some approximation technique must be employed which will allow for an approximate yet representative solution. One method used in cases where the fluid depth is large compared to a typical wavelength was presented by Stokes (1847) for surface waves. This method, known as the 'Stokes expansion', was extended by Hunt (1961) to include interfacial waves.

The Stokes expansion technique involves the use of expansions about the mean water level $\bar{\eta} = 0$. Each term in the equations of motion is expanded and compared in magnitude to other expansion terms. Those terms of like order and those of lower order form the equations of motion which when solved give a solution valid to that order. The success of this expansion procedure depends on the

property that the ratio of a typical non-linear term to a linear term is in deep water of the order of the wave slope. This condition insures that the expansions are convergent and allows that non-linear terms can be regarded as perturbations on the linear solution.

In applying the Stokes expansion, we expand Φ, $\underset{\sim}{v}$, and η in powers of an ordering parameter ϵ,

$$\Phi = \epsilon\Phi_1 + \epsilon^2\Phi_2 + \epsilon^3\Phi_3 + \cdots, \tag{A.2.1}$$

$$\underset{\sim}{v} = \epsilon\underset{\sim}{v}_1 + \epsilon^2\underset{\sim}{v}_2 + \epsilon^3\underset{\sim}{v}_3 + \cdots, \tag{A.2.2}$$

$$\eta = \epsilon\eta_1 + \epsilon^2\eta_2 + \epsilon^3\eta_3 + \cdots \tag{A.2.3}$$

where ϵ, as a requirement for convergence, is of the order of the wave slope and is given to be

$$\epsilon = \frac{ak}{\pi} = \frac{2a}{L} . \tag{A.2.4}$$

These parameterized forms of Φ, $\underset{\sim}{v}$, and η are then substituted into the non-linearized form of the equations of motion (2.23) through (2.29) of Chapter II. Each parameterized term is then expanded in a Maclaurin series about the mean water level $z = 0$.

If F is a function of η, such a Maclaurin series expansion of F about $z = 0$ will be

$$F(\eta) = F(0) + \eta\frac{\partial F}{\partial z}\bigg|_{z=0} + \frac{\eta^2}{2!}\frac{\partial^2 F}{\partial z}\bigg|_{z=0} + \cdots \tag{A.2.5}$$

The expanded terms in each equation are now equated according to powers of ϵ. The terms proportional to ϵ give the first-order approximation to the general wave equations. The terms proportional to ϵ^2 give the second-order approximation and so on.

We are restricting our attention in this work to the second-order theory and will therefore neglect higher order terms. The convergence of the Stokes expansion technique for progressive interfacial waves has been proven by Hunt (1961) and others and will not be explored here. Due to the tedious nature of the Stokes method, only the results of the expansion will be presented. The geometry and notation conform to that used in Chapter II.

$$\nabla^2 \Phi_i = 0 \qquad \text{for } i = 1, 2. \qquad \text{(A.2.6)}$$

The kinematic boundary condition at the interface is to first-order

$$\frac{\partial \eta_1'}{\partial t} = -\frac{\partial \Phi_1'}{\partial z} = \frac{\partial \Phi_1''}{\partial z} \qquad \text{at } z = 0, \qquad \text{(A.2.7)}$$

and to second-order

$$\frac{\partial \eta_2}{\partial t} = -\frac{\partial \Phi_2'}{\partial z} - \underset{\sim}{v}_1' \cdot \underset{\sim\sim}{\nabla} \eta_1' - \eta_1' \frac{\partial^2 \Phi_1'}{\partial z^2}$$

$$= -\frac{\partial \Phi_2''}{\partial z} - \underset{\sim}{v}_1'' \cdot \underset{\sim\sim}{\nabla} \eta_1'' - \eta_1' \frac{\partial^2 \Phi_1''}{\partial z^2} \qquad \text{at } z = 0. \qquad \text{(A.2.8)}$$

The dynamic boundary condition at the free surface is to first-order

$$\frac{\partial^2 \Phi_1'}{\partial t^2} = - g \frac{\partial \Phi_1'}{\partial z} \qquad \text{at } z = h', \qquad \text{(A.2.9)}$$

and to second-order

$$\frac{\partial^2 \Phi_2'}{\partial t^2} + \eta_1' \frac{\partial}{\partial z} \frac{\partial^2 \Phi_1'}{\partial t^2} + g \frac{\partial \Phi_2'}{\partial z} + g\eta_1' \frac{\partial^2 \Phi_1'}{\partial z^2} + \frac{\partial |\underset{\sim}{v}_1'|^2}{\partial t} = 0 \quad \text{at } z = h'. \qquad \text{(A.2.10)}$$

The kinematic boundary condition to be satisfied at the bottom $z = -h''$ is to first- and second-order

$$\frac{\partial \Phi_i''}{\partial z} = 0 \qquad \text{at } z = -h''; \; i = 1, 2. \qquad \text{(A.2.11)}$$

The pressure boundary condition at the interface is to first-order

$$\rho' \left(\frac{\partial \Phi_1'}{\partial t} - g\eta_1\right) = \rho'' \left(\frac{\partial \Phi_1''}{\partial t} - g\eta_1\right) \qquad \text{at } z = \eta, \qquad \text{(A.2.12)}$$

and to second-order

$$\rho' \left(\frac{\partial \Phi_2'}{\partial t} + \eta_1' \frac{\partial \Phi_1'}{\partial t} + \frac{|\underset{\sim}{v}_1'|^2}{2} - \eta_2\right) =$$

$$\rho'' \left(\frac{\partial \Phi_2''}{\partial t} + \eta_1'' \frac{\partial \Phi_1''}{\partial t} + \frac{|\underset{\sim}{v}_1''|^2}{2} - \eta_2\right) \qquad \text{at } z = \eta. \qquad \text{(A.2.13)}$$

APPENDIX III

RICHARDSON NUMBER

The Richardson number is defined to be the square of the ratio of the Brunt-Vaisala frequency to the rate of shear at a specified point in a fluid flow.

$$R_i = -\left(\frac{g}{\rho_0}\frac{\partial \bar{\rho}_{pot}}{\partial z}\right) \Big/ \left(\frac{dU}{dz}\right)^2 = \frac{N^2(z)}{(U'(z))^2} \qquad \text{(A. 3. 1)}$$

where

$$\frac{\partial \bar{\rho}_{pot}}{\partial z} = \frac{\partial \bar{\rho}}{\partial z} + g^2/c^2 \qquad \text{(A. 3. 2)}$$

where $N(z)$ is the Brunt-Vaisala frequency, U is the magnitude of the horizontal component of the velocity of the flow, $\bar{\rho}_{pot}$ is the mean potential density of the fluid, and ρ_0 is the density at $z = 0$. Howard (1961) shows that a Richardson number, $R_i = 1/4$, is the minimum condition which is sufficient for stability everywhere in an arbitrary shearing flow. A complete review of Richardson number theory can be found in Drazin and Howard (1966).

APPENDIX IV

BOUSSINESQ APPROXIMATION

The Boussinesq approximation is a technique employed to simplify the equations of motion of a flow. This simplification, if valid, enables one to readily obtain solutions to the approximate wave equations. In particular, the Boussinesq approximation, B.a., consists of applying three assumptions to the system under consideration. First, the variation of pressure on a fluid element is assumed to be strictly a function of depth. Thus, the effects of molecular diffusion and (near the free surface) of radiative transfer are neglected. Secondly, as a direct consequence of this first assumption, the fluid is taken to be incompressible,

$$\nabla \cdot \underset{\sim}{v} = 0 . \qquad \text{(A.4.1)}$$

Thirdly, the B.a. requires that the difference between the actual density of a fluid and the density of a similar fluid in a reference state (subscript r) of constant entropy and salinity at rest relative to the rotating earth is negligibly small. In considerations dealing with the ocean, this leads to the assumption that neglecting the effects of surface heating and cooling and the resultant convective mixing, the reference density ρ_r can be assumed a constant ρ_0. The pressure p under these assumptions is, then, the difference between the actual

and the hydrostatic pressure in an ocean at rest with constant density.

Under the B.a., the Navier-Stokes equation reduces from:

$$\rho \frac{d\underset{\sim}{v}}{dt} + \rho \underset{\sim}{\Omega} \times \underset{\sim}{v} + \underset{\sim}{\nabla} P - (\rho - \rho_r) \underset{\sim}{g} = \underset{\sim}{f} \qquad (A.4.2)$$

where $P = p - p_r$ and $\underset{\sim}{f}$ is the resultant of all other forces on a unit volume of the fluid to:

$$\frac{d\underset{\sim}{v}}{dt} + \underset{\sim}{\Omega} \times \underset{\sim}{v} + \frac{1}{\rho_0} \underset{\sim}{\nabla} p - \frac{\rho - \rho_0}{\rho_0} \underset{\sim}{g} = \nu \nabla^2 \underset{\sim}{v} \qquad (A.4.3)$$

where $\nu = \mu / \rho_0$ is the kinematic viscosity.

A more extensive discussion of the Boussinesq approximation is presented in Phillips (1966). Its application to a compressible fluid can be found in Spiegel and Veronis (1960).

It is always necessary to examine the effects of making the B.a. and in so doing establish the validity of its use.

The first effect of using the B.a. is that it may modify the dispersion relation as a result of the simplification of the linearized form of equation (3.1). This is discussed in Thorpe (1968). In general it is impossible to predict whether or not the B.a. may be valid without examining the solution of the governing Sturm-Liouville equation.

The second effect of the B.a. is that it may modify the finite amplitude solution. This work was first done by Long (1965) and was extended by Thorpe (1968). Their results indicate that, if the terms neglected by making the B.a. are significant, they will alter

the wave amplitude and perhaps affect the phase speed of the waves, but will not change the wave shape. The shape of the internal waves will be affected, however, when higher order expansion terms become important. The importance of these neglected and higher order terms is again not obvious from a general analysis. Long (1965) and Benjamin (1966) suggest that for extreme values of the ratio of the fluid depth divided by the wavelength, the B.a. may become invalid.

As indicated by Thorpe (1968), the B.a. is valid for the linear density profile bounded in amplitude as required by the rigid horizontal boundary assumption. However, each density profile must be examined individually to determine if the B.a. is valid within the range of wave amplitudes to be considered. The $\rho_0=\rho_0(0)(1-\Delta \tanh az)$ density profile is an example wherein the B.a. is invalid for the first mode regardless of amplitude yet valid for higher modes within a finite wave height range.

APPENDIX V

TSUNAMI GEK RESPONSE

Tsunamis fall under the class of long-crested surface waves. The GEK theory for such waves can be found in Longuet-Higgins, Stern, and Stommel (1954).

Let the Cartesian axes be taken with the origin in the mean free surface as shown in Figure 4.

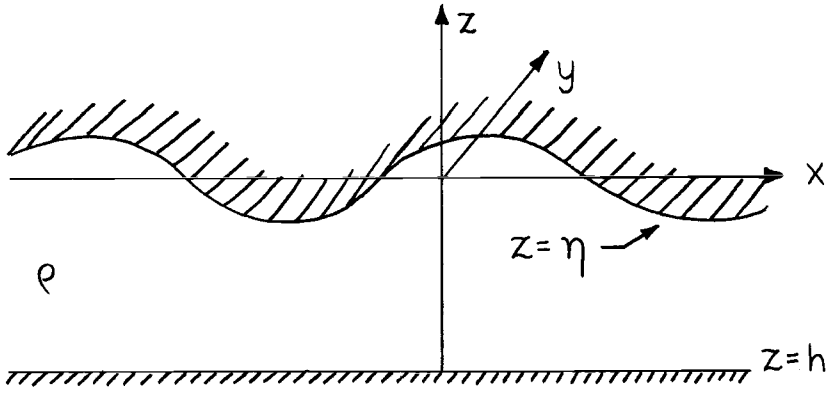

Figure 4. Long crested wave geometry.

The x-axis is in the direction of propagation, the y-axis is parallel to the wave crests, and the z-axis is vertically upwards.

We will restrict ourselves to the case of infinitely long-crested waves at the surface of a finite but deep ocean with uniform electrical resistivity ρ.

It can be shown that long-crested waves at the sea surface of

the form,

$$\eta = a \cos(kx - \sigma t) , \qquad (A.5.1)$$

will generate a towed electrode GEK signal of the form

$$\text{GEK Signal} = - H_z \ell a k c \coth kh \cos(kx - \sigma t) + $$

$$+ H_x \ell a k c \sin(kx - \sigma t) \qquad (A.5.2)$$

where a = wave amplitude, h = depth of the bottom, ℓ = electrode separation PQ, H_x and H_z are the horizontal and vertical components of the Earth's magnetic field respectively, $ck = \sigma$, and

$$c^2 = \frac{g}{k} \tanh kh . \qquad (A.5.3)$$

Table 2 lists the predicted values of towed electrode GEK signal components for tsunamis of one meter amplitude in a region where $H_x = H_z = 0.1$ oersteds. The electrode separation PQ is taken to be 100 meters, $h = 1500$ meters, and $g = 980.62$ cm/sec^2.

The natural range of tsunami periods is between 15 to 20 minutes. Tsunami wave heights are of the order of a few feet at most in deep water. Therefore, most tsunamis fall within the wave number range of k less than $k = 1 \times 10^{-3}$ m^{-1} for which, as discussed in Appendix I the above GEK theory does not apply. The values in Table 2 for $k = 1 \times 10^{-4}$ m^{-1} and $k = 5 \times 10^{-4}$ m^{-1} are in this respect invalid, but give a rough indication of the expected magnitude of the GEK components.

Table 2. Tsunami Towed Electrode GEK Components

k (m^{-1})	Period (sec)	L (m)	c (m/sec)	H_x Term (mv/100m/0.1 oe)	H_z Term (mv/100m/0.1 oe)
1×10^{-2}	19.92	623.82	31.31	0.3131	0.3131
1×10^{-3}	66.21	6.24×10^{3}	94.21	0.0942	0.1041
1×10^{-4}	516.27	6.24×10^{4}	120.83	0.0121	0.0812
5×10^{-5}	1029.47	1.25×10^{5}	121.19	0.0060	0.0813

APPENDIX VI

EFFECTS OF NATURAL PHENOMENA ON GEK OPERATION

A GEK theory should always be examined in terms of the assumptions made during its development. This is necessary in order to determine and account for the effect of conditions found in nature which differ from the theoretical model. Only then can experimental measurements be properly interpreted to provide useful information. Thus, it is the purpose of this appendix to discuss recent findings on the effect of natural phenomena on GEK signals and to point out to the experimentalist which variables need to be monitored during a GEK operation to aid in the interpretation of his results.

The assumption of a non-conducting sea bed has been investigated by Stommel (1948), Longuet-Higgins (1949), Longuet-Higgins, Stern, and Stommel (1954), and Glasko and Sveshnikov (1961). They agree that in deep water the sea bed can be regarded as an insulator. Such an assumption will introduce an error of the order of

$$\epsilon = \sigma_1/\sigma_0 \qquad \text{(A. 6. 1)}$$

where σ_1 = sea floor conductivity and σ_0 is the sea water conductivity. Hughes (1962), on the other hand, emphasizes that in shallow water the resistivity of the sea bed critically influences the electric current flow and hence the electrode sensitivity.

Variation of the conductivity of sea water has been analyzed with respect to its GEK effects by Longuet-Higgins, Stern, and Stommel (1954). They show that the vertical variation of conductivity in the deep ocean is mainly influenced by the temperature whereas in estuaries the salinity is the governing factor. These variations of resistivity act to reduce the measured signals. For a two-fluid system in the deep ocean, a relative error introduced by the resistivity ρ_1 being different from resistivity ρ_2 is of the order of

$$\epsilon = \frac{\rho_2 - \rho_1}{\rho_1} \frac{h'}{h''}$$

where h' and h'' are the depths of the upper layer and lower layer respectively. In the deep ocean, the factor $(\rho_2-\rho_1)/\rho_1$ varies from 0.0 in polar regions to 0.3 in the tropics leaving most of the error due to h'/h''. The horizontal changes in the conductivity of sea water were found to be negligible by Sanford (1967).

The sensitivity of the Ag-AgCl electrodes most commonly used in GEK work is presented in detail by Sanford (1967). Salinity and temperature changes will produce cell potentials of the order of $-2.5\ \mu v/‰/^{o}K$. This figures to be approximately -0.5 mv/‰ and $+0.36$ mv/^{o}C at 37‰ and 22^{o}C. Sea water oxygen content and pressure difference effects are negligible within the normal oceanic range of these variables.

Ship speed and heading in relation to the direction of propagation of the wave or current system under inspection is of prime importance in determining the signal strength. As mentioned in Chapter I, electrode alignment in the direction of wave propagation will yield no signal. A perpendicular heading will produce a maximum signal. Intermediate directions of electrode travel are discussed in von Arx (1950) and Longuet-Higgins, Stern, and Stommel (1954). Moreover, cable droop effects can be large as indicated by Knauss and Reid (1957) and should be experimentally determined for particular cable-electrode arrangements.

Surface waves (see Appendix V) can produce GEK responses which, though different in period, are of magnitudes similar to internal wave signals. Therefore, a knowledge of the major surface wave heights and periods is desirable to aid in distinguishing surface wave responses from internal wave responses. In the general case wherein the period of the internal wave is not known a priori, knowledge of the sea surface state is a necessity. The secondary effect on waves of the Lorentz body force produced by the induced electric currents can be regarded as insignificant as verified by Williams (1930).

All potential sources of interference from shipboard electrical and radar systems must be inspected. In addition, an understanding of the in situ large scale flow pattern must be obtained, as Larsen (1966) has calculated that flows in the order of tens of kilometers in

length can affect the local Earth's magnetic field. Perhaps of greater significance is the possible effect of Earth currents generated by geomagnetic disturbances. The analyses of Novysh (1965), Fonarev (1968), Runcorn (1964), and Fonarev and Novysh (1965) point out that aside from the initial effect of varying the local magnetic field, these disturbances can produce telluric currents which should not be overlooked in evaluating GEK measurements. Their determination of the effects of the major geomagnetic disturbances is as follows:

Long period (27-day, semiannual, annual, two-year, 11-year, and secular) geomagnetic variations always generate telluric currents of less than the 1.0 mv/km GEK instrument sensitivity and are thereby ignorable (Fonarev, 1968).

Solar-diurnal variations with a period of 24 hours are of two types, both of which are significant. The first type are the relatively quiet day variations (S_q) which come from ionospheric electric currents. S_q disturbances vary with latitude and season producing GEK errors of the order of tenths or units of mv/km. Forbush and Casaverde (1961) established that within a 600 km band about the equator, the equatorial electrojet accounts for about half the total range of S_q variation in the Earth's magnetic field. The second type of solar-diurnal variation are the disturbed day variations (S_D). These are the result of magnetic storms and consist of a latitude-dependent oscillation with one maximum and one minimum per day.

The S_D can generate from one half unit to tens of units of mv/km.

Bay-disturbances, so named because of their shape, are due to band-like currents at 100-150 km altitude at a latitude of 70^{o} in the auroral zone. Bays occur 10 to 40 times per year and induce telluric currents of the order of tens of mv/km. Bay disturbances, though polar in origin, extend over vast areas sending telluric currents even to the equator.

Electromagnetic storms are the strongest of all sources of magnetic interference. There are two types: the polar storm and an in-phase disturbance encompassing the entire globe known as a global storm. The annual number of global storms varies from 10 to 40 depending on solar activity. The induced telluric currents will be of the order of tens of mv/km in low latitudes and of the order of hundreds of mv/km in the high latitudes. The GEK record takes on a saw-tooth appearance during such storms and is easily recognized.

Short period pulsations (SPP) constitute the last geomagnetic variation to be considered. These micropulsations are a superposition of quasi-harmonic oscillations appearing as individual trains lasting 3-40 minutes or as stable pulsations lasting a number of hours. The periods of the oscillations vary from 0.2 to 600 secs. SPP with periods of a few minutes generate GEK errors of tens of mv/km, particularly in polar regions. Pulsations with periods of a few to tens of seconds generate GEK readings of the order of hundredths to a

few mv/km. These latter SPP can, therefore, generate GEK readings identical to those produced by surface and internal waves. In view of this, the simultaneous recording of the local geomagnetic field via a shipboard magnetometer is essential.